

Ultrathin Binary Grafted Polymer Layers with Switchable Morphology

Melburne C. LeMieux,[†] Duangrut Julthongpiput,^{†,§} Kathryn N. Bergman,[†] Pham Duc Cuong,[‡] Hyo-Sok Ahn,[‡] Yen-Hsi Lin,[†] and Vladimir V. Tsukruk^{*,†}

Materials Science & Engineering Department, Iowa State University, Ames, Iowa 50011, and Tribology Research Center, Korean Institute of Science and Technology, Seoul 136-791, South Korea

Received June 17, 2004. In Final Form: August 23, 2004

Polymer surface layers comprised of mixed chains grafted to a functionalized silicon surface with a total layer thickness of *only* 1–3 nm are shown to exhibit reversible switching of their structure. Carboxylic acid-terminated polystyrene (PS) and poly (butyl acrylate) (PBA) were chemically attached to a silicon surface that was modified with an epoxysilane self-assembled monolayer by a “grafting to” routine. While one-step grafting resulted in large, submicron microstructures, a refined, two-step sequential grafting procedure allowed for extremely small spatial dimensions of PS and PBA domains. By adjusting the grafting parameters, such as concentration of each phase and molecular weight, very finely structured surfaces resulted with roughly 10-nm phase domains and less than 0.5-nm roughness. Combining the glassy PS and the rubbery PBA, we implemented a design approach to fabricate a mixed brush from two immiscible polymers so that switching of the surface nanomechanical properties is possible. Post-grafting hydrolysis converted PBA to poly(acrylic acid) to amplify this switching in surface wettability. Preliminary tribological studies showed a difference in wear behavior of glassy and rubbery surface layers. Such switchable coatings have practical applications as surface modifications of complex nanoscale electronic devices and sensors, which is why we restricted total thickness for potential nanoscale gaps.

Introduction

Flexible polymer chains have long been known to respond and conform to subtle local changes in pH, temperature, and solvent quality. Thus, polymer surface modification, which inherently provides the ability to control and change surface composition allowing on-demand properties, is becoming increasingly significant for practical applications in fields such as nanoscale lubrication, sensing and biocompatibility,^{1–8} or the exciting advancement of functional carbon nanotube

devices.^{9–12} Polymer brush layers are considered ideal choices in such applications for several reasons. They are chemically tethered to the surface at one end, virtually any chemistry can be designed into the layer depending on intended surface interactions, and the high grafting density combined with uniformity in composition and structure allows the *entire* surface to *quickly* respond to local environmental stimuli. These unique qualities have led to intense theoretical and experimental development of polymer brush systems.^{13–17}

Aside from responsive coatings, a parallel approach is the development of nanocomposite polymer layers with heterogeneous surface properties. The design of molecular coatings with controllable size and shape of novel nanostructures is an important topic for nanotemplates and microelectronics.^{18,19} Other approaches have used im-

* Author to whom correspondence should be addressed. E-mail: vladimir@iastate.edu.

[†] Iowa State University.

[‡] Korean Institute of Science and Technology.

[§] Current address: Polymers Division, Stop 8542, NIST, 100 Bureau Drive, Gaithersburg, MD 20899-8542.

(1) Ionov, L.; Minko, S.; Stamm, M.; Gohy, J.-F.; Jérôme, R.; Scholl, A. *J. Am. Chem. Soc.* **2003**, *125*, 8302. Luzinov I.; Minko, S.; Tsukruk, V. V. *Prog. Polym. Sci.* **2004**, *29*, 635.

(2) Bliznyuk, V. N.; Everson, M. P.; Tsukruk, V. V. *J. Tribology* **1998**, *120*, 489. Tsukruk, V. V.; Bliznyuk, V. N. *Langmuir* **1998**, *14*, 446. Sidorenko, A.; Houphouet-Boigny, C.; Villavicencio, O.; McGrath, D. V.; Tsukruk, V. V. *Thin Solid Films* **2002**, *410*, 147. Peleshanko, S.; Sidorenko, A.; Larson, K.; Villavicencio, O.; Ornatska, M.; McGrath, D. V.; Tsukruk, V. V. *Thin Solid Films* **2002**, *406*, 233. Ahn, H.; Julthongpiput, D.; Kim, D. I.; Tsukruk, V. V. *Wear* **2003**, *255*, 801. Tsukruk, V. V.; Sidorenko, A.; Yang, H. *Polymer* **2002**, *43*, 1695. Sidorenko, A.; Julthongpiput, D.; Luzinov, I.; Tsukruk, V. V. *Tribol. Lett.* **2002**, *12*, 101.

(3) Ito, Y.; Ochiai, Y.; Park, Y. S.; Imanishi, Y. *J. Am. Chem. Soc.* **1997**, *119*, 1619.

(4) Galaev, I.; Mattiasson, B. *Trends Biotechnol.* **1999**, *17*, 335.

(5) Jones, D. M.; Smith, R. R.; Huck, W. T. S.; Alexander, C. *Adv. Mater.* **2002**, *14*, 1130.

(6) Aksay, I. A.; Trau, M.; Manne, S.; Honma, I.; Yao, N.; Zhou, L.; Fenter, P.; Eisenberger, P. M.; Gruner, S. M. *Science* **1996**, *273*, 892.

(7) Dean, D.; Seog, J.; Ortiz, C.; Grodzinsky, A. *J. Langmuir* **2003**, *19*, 5526.

(8) Rixman, M. A.; Dean, D.; Ortiz, C. *Langmuir* **2003**, *19*, 9357.

(9) Qin, S. H.; Oin, D. Q.; Ford, W. T.; Resasco, D. E.; Herrera, J. E. *J. Am. Chem. Soc.* **2004**, *126*, 170.

(10) Gomez, F. J.; Chen, R. J.; Wang, D. W.; Waymouth, R. M.; Dai, H. *J. Chem. Commun.* **2003**, 190.

(11) Viswanathan, G.; Chakrapani, N.; Yang, H. C.; Wei, B. Q.; Chung, H. S.; Cho, K. W.; Ryu, C. Y.; Ajayan, P. M. *J. Am. Chem. Soc.* **2003**, *125*, 9258.

(12) Artyukhin, A. B.; Bakajin, O.; Stroeve, P.; Noy, A. *Langmuir* **2004**, *20*, 1442.

(13) Alexander, S. J. *J. Phys.* **1977**, *38*, 977.

(14) de Gennes, P. G. *Macromolecules* **1980**, *13*, 1069.

(15) Karim, A.; Tsukruk, V. V.; Douglas, J. F.; Satija, S. K.; Fetters, L. J.; Reneker, D. H.; Foster, M. D. *J. Phys. II* **1995**, *5*, 1441. Tsukruk, V. V. *Prog. Polym. Sci.* **1997**, *22*, 247. Tsukruk, V. V. *Adv. Mater.* **1998**, *10*, 253.

(16) Zhao, B.; Brittain, W. J. *Prog. Polym. Sci.* **2000**, *25*, 677. Zhao, B.; Brittain, W. J. *J. Am. Chem. Soc.* **1999**, *121*, 3557. Zhao, B.; Brittain, W. J.; Zhou, W. S.; Cheng, S. Z. D. *J. Am. Chem. Soc.* **2000**, *122*, 2407.

(17) Wittmer, J.; Johner, A.; Joanny, J. F. *Colloids Surf., A* **1994**, *86*, 85.

(18) Sidorenko, A.; Tokarev, I.; Minko, S.; Stamm, M. *J. Am. Chem. Soc.* **2003**, *125*, 12211.

miscible polymer blends and physisorbed layers, but dewetting is a prevalent problem in thin homopolymer blend films, and only chemisorbed layers possess practical robustness and stability. Chemically attached block copolymers have been widely exploited for this purpose, as the periodicity and control of domains is well understood in these systems.^{20,21} Recent work has focused on using block copolymer systems as protective or lubricating coatings for surfaces with repeated nanoscale contacts. It has been shown that triblock copolymers of poly[styrene-*b*-(ethylene-*co*-butylene)-*b*-styrene] (SEBS) formed fine domains of mechanically stiff PS and rubbery PEB chains with 30-nm interdomain spacing in a thin (9 nm) polymer film.²² When this reinforced rubber layer was capped with a hard top layer, the resulting triplex coating provided an effective means of energy dissipation due to the large reversible elastic deformation possible, along with preventing penetration of sharp contacts to the surface via the hard top layer.²³ The main drawback with this coating is that it was relatively thick (within 20–50 nm), although it displayed exceptional surface nanomechanical heterogeneity and tribological properties.^{24,25} Building on this approach, PS homopolymer was blended with SEBS to form a mechanically heterogeneous, non-dewetting film with the thinnest film still being around 10 nm thick.

Merging the responsive and sensing properties of grafted homopolymer brushes with the vast array of nanostructures and phase separations capable in block copolymer systems into a single polymer film is possible in binary (mixed) polymer brush layers.²⁶ In the case of binary brushes, the variety of surface morphologies possible greatly increases depending upon the chemical composition. Surface composition, and hence, properties such as surface energy, adhesion, friction, and wettability have the possibility of being “tuned” to the necessary state.^{27,28} Current theory predicts, ideally, either complete lateral or complete vertical (layered) segregation of the two components within the binary assembly.^{29–32}

Synthesis of binary brushes is a challenging issue with several factors considered. First, each homopolymer brush must be chemically attached to the substrate either with a grafting to or a grafting from approach. In general, grafting to is a more simple process, although it is kinetically limited.²² On the other hand, brushes grown from the surface (grafting from) are more dense and thicker, with the major drawbacks of having complicated

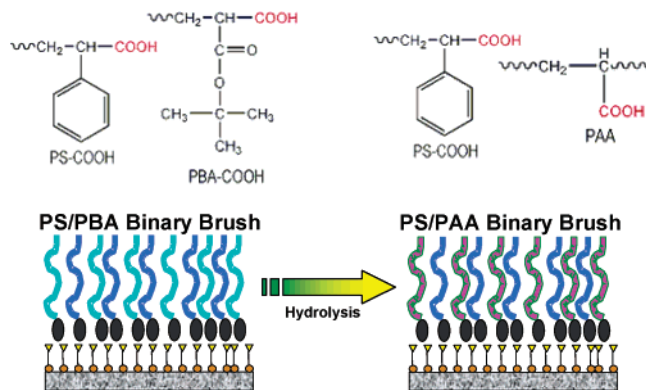


Figure 1. Chemical formulas for PBA, PS, and PAA (top) along with schematics (bottom) of the binary brushes before and after hydrolysis.

synthesis and characterization procedures.^{33–35} Second, to produce smaller, intriguing phases, two incompatible polymers should be immobilized randomly on the surface, which should be done in a two-step (sequential) grafting scheme to avoid agglomeration and dewetting. Zhao reported synthesis of randomly mixed brushes by having mixed SAMs (coadsorbed from one solution) on the surface, but the phase separation of the mixed SAMs can be a serious issue.³⁶ In another publication, to avoid preferential adsorption, a double-branched SAM was used that was selective to each monomer, with the resulting surface morphology of the mixed brush showing nanoscale domain structure.³⁷ Recently, Julthongpipit et al. synthesized a novel Y-shaped brush layer in which two incompatible polymer “arms” were attached at a single focal point, which in turn grafted to the surface.^{38,39} The spatial constraints led to never-before-observed nanoscale phase separations of pinned micelles and craterlike structures. Poly(methyl acrylate) and fluorinated polystyrene (PSF) binary brushes were sequentially grown from the surface and could be completely and reversibly switched between the glassy, low-energy PSF on the topmost layer to the rubbery PMA occupying the top layer as a function of solvent exposure.⁴⁰ This resulted in having a surface with 2-nm RMS roughness, a roughly 1-GPa elastic modulus in one state, and switching to a surface with a 30-nm RMS roughness and a 40-MPa elastic modulus with two times higher adhesion in a *single* polymer film with total thicknesses ranging from 50 to 150 nm.^{40,41} To date, this issue has not been addressed in sequentially grafted mixed brushes with total thickness less than 10 nm.

In this paper, we demonstrate how ultrathin (less than 3 nm) and stable nanocomposite-grafted surface layers can be obtained from dissimilar functionalized polymers (Figure 1). For these layers, we observed the microstructural reorganization upon exposure to selective solvents for each component. Postgrafting hydrolysis was performed to induce amphiphilicity in these binary brushes.

(19) Bhushan, B., Ed. *Tribology Issues and Opportunities in MEMS*; Kluwer Academic Publishers: Dordrecht, The Netherlands, 1997.

(20) Bates, F. S.; Fredrickson, G. H. *Annu. Rev. Phys. Chem.* **1990**, *41*, 525.

(21) Krausch, G.; Magerle, R. *Adv. Mater.* **2002**, *14*, 1579.

(22) Luzinov, I.; Julthongpipit, D.; Tsukruk, V. V. *Macromolecules* **2000**, *33*, 7629.

(23) Tsukruk, V. V.; Ahn, H. S.; Kim, D.; Sidorenko, A. *Appl. Phys. Lett.* **2002**, *80*, 4825.

(24) Tsukruk, V. V.; Sidorenko, A.; Gorbunov, V. V.; Chizhik, S. A. *Langmuir* **2001**, *17*, 6715.

(25) Sidorenko, A.; Ahn, H. S.; Kim, D. I.; Yang, H.; Tsukruk, V. V. *Wear* **2002**, *252*, 946.

(26) Sidorenko, A.; Minko, S.; Schenk-Meuser, K.; Duschner, H.; Stamm, M. *Langmuir* **1999**, *15*, 8349.

(27) Minko, S.; Patil, S.; Datsyuk, V.; Simon, F.; Eichhorn, K. J.; Motornov, M.; Usov, D.; Tokarev, I.; Stamm, M. *Langmuir* **2002**, *18*, 289.

(28) Minko, S.; Usov, D.; Goreshnik, E.; Stamm, M. *Macromol. Rapid. Comm.* **2001**, *22*, 206.

(29) Soga, K. G.; Zuckermann, M. J.; Guo, H. *Macromolecules* **1996**, *29*, 1998.

(30) Marko, J. F.; Witten, T. A. *Phys. Rev. Lett.* **1991**, *66*, 1541.

(31) Müller, M. *Phys. Rev. E* **2002**, *65*, 30802.

(32) Minko, S.; Müller, M.; Usov, D.; Scholl, A.; Froeck, C.; Stamm, M. *Phys. Rev. Lett.* **2002**, *88*, 5502.

(33) Boven, G.; Oosterling, M. L. C. M.; Challa, G.; Schouten, A. J. *Polymer* **1990**, *31*, 2377.

(34) Prucker, O.; Ruhe, J. *Macromolecules* **1998**, *31*, 592.

(35) Prucker, O.; Ruhe, J. *Macromolecules* **1998**, *31*, 602.

(36) Zhao, B. *Polymer* **2003**, *44*, 4079.

(37) Zhao, B.; He, T. *Macromolecules* **2003**, *36*, 8599. Zhao, B.; Haasch, R. T.; MacLaren, S. *J. Am. Chem. Soc.* **2004**, *126*, 6124.

(38) Julthongpipit, D.; Lin, Y. H.; Teng, J.; Zubarev, E. R.; Tsukruk, V. V. *J. Am. Chem. Soc.* **2003**, *125*, 15912.

(39) Julthongpipit, D.; Lin, Y. H.; Teng, J.; Zubarev, E. R.; Tsukruk, V. V. *Langmuir* **2003**, *19*, 7832.

(40) Lemieux, M.; Usov, D.; Minko, S.; Stamm, M.; Shulha, H.; Tsukruk, V. V. *Macromolecules* **2003**, *36*, 7244.

(41) Lemieux, M.; Minko, S.; Usov, D.; Stamm, M.; Tsukruk, V. V. *Langmuir* **2003**, *19*, 6126.

Table 1. Grafting Conditions for Different Samples

sample	SiO ₂ thickness (nm)	epoxysilane thickness (nm)	binary brush step 1 (PBA grafting)	binary brush step 2 (PS grafting)
1	1.10	0.75 ± 0.04	PBA 1 = 0.58 nm 20 min at 50 °C 0.5% PBA in toluene	PBA 1 + PS 1 = 1.95 nm 18 h at 150 °C 2% PS 1 in toluene
2	1.10	0.75 ± 0.04	PBA 1 = 0.94 nm 20 min at 70 °C 0.5% PBA in toluene	PBA 1 + PS 1 = 3.02 nm 18 h at 150 °C 2% PS 1 in toluene
3	1.10	0.72 ± 0.04	PBA 1 = 0.87 nm 20 min at 50 °C 0.5% PBA in toluene	PBA 1 + PS 2 = 2.79 nm 18 h at 150 °C 2% PS 2 in toluene
4	1.10	0.72 ± 0.04	PBA 1 = 0.90 nm 20 min at 70 °C 0.5% PBA in toluene	PBA 1 + PS 2 = 3.56 nm 18 h at 150 °C 2% PS 2 in toluene

Here, we discuss how molecular weight and type of grafting affect the resulting surface morphology and report preliminary results on their surface tribological properties.

Experimental Section

Materials and Methods. Carboxyl acid-terminated polystyrene (M_n : PS 1 = 4200 g/mol; PS 2 = 9700 g/mol) with very narrow polydispersity ($M_w/M_n = 1.08$ for PS 1 and PS 2) and carboxyl acid-terminated poly(butyl acrylate) (M_n : PBA 1 = 6500 g/mol with $M_w/M_n = 1.06$) polymers (Figure 1) were obtained from Polymer Source, Inc. The epoxysilane-anchoring layer is (3-glycidoxypropyl)trimethoxysilane (Gelest, Inc.) and is fabricated according to the established procedure.^{42,43} Anhydrous toluene was obtained from Aldrich, further dried with sodium, and stored in a nitrogen-filled glovebox with relative humidity not exceeding 2%. The silicon wafer {100} substrates were first cleaned in an ultrasonic bath for 30 min, placed in a hot (90 °C) bath (3:1 concentrated sulfuric acid: 30% hydrogen peroxide) for 1 h, and then rinsed with Nanopure water (18 M Ω cm, Nanopure). Regarding the polymer solutions, we used two different approaches for grafting: concurrent grafting when a surface layer formed from the two mixed polymers at once and sequential (one polymer after another) grafting. In the latter approach, after each grafting step, the sample was vigorously rinsed with toluene and additionally washed in an ultrasonic toluene bath to remove all ungrafted chains. The solutions were prepared in various concentrations of toluene ranging from 0.5 to 2.0 wt% polymer (Table 1) and spin coated onto the epoxysilane-modified silicon wafers at 3000 rpm. The sample was then annealed to facilitate grafting between the epoxy and carboxyl acid groups,⁴⁴ then spin coated with the second polymer (for the sequential grafting approach), and then annealed again. All sample preparation was carried out under vacuum conditions. For the sequential approach, when PS was grafted as the first step (first polymer), unstable layers formed, thus, PBA was always grafted as the first polymer. Since PBA and PS have similar water contact angles, postgrafting hydrolysis was conducted to completely replace the PBA polymer with poly(acrylic acid) (PAA), which made the binary brush amphiphilic in nature with hydrophobic PS chains and hydrophilic PAA chains (Figure 1). The brush was hydrolyzed in a mixture of 30% tetrahydrofuran and 70% trifluoroacetic acid for 48 h, rinsed with Nanopure water and toluene, and then sonicated. All sample preparation was done inside a Class 100 Cleanroom facility.

All thickness measurements were obtained with a COMPEL Automatic Ellipsometer (InOm Tech, Inc.) with an incident angle of 70°. ⁴⁵ The thickness of the spin coated films after each step (before annealing) was 36 ± 3 nm. Independent epoxysilane SAM thicknesses were measured before polymer grafting to be

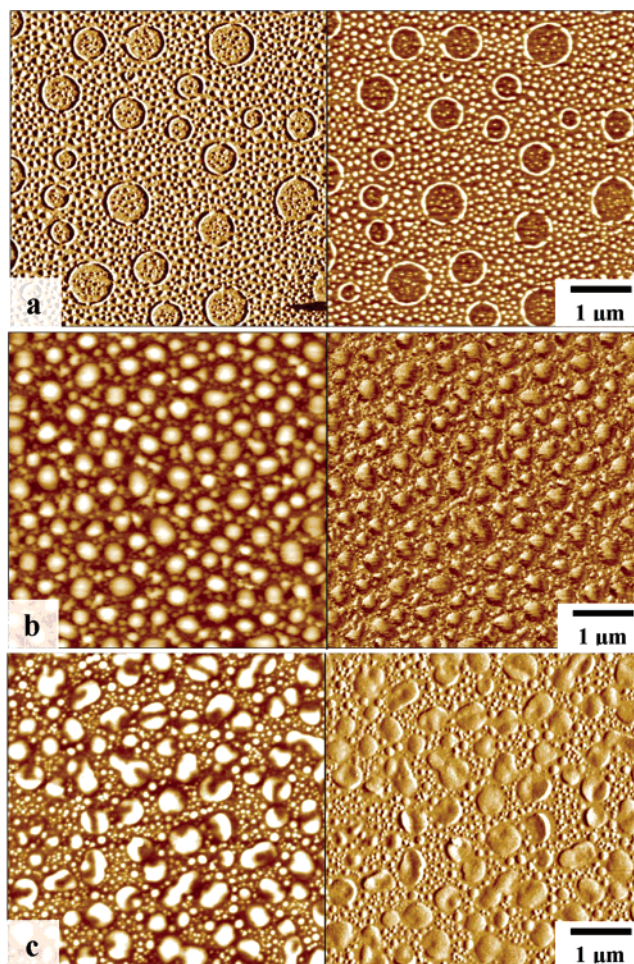


Figure 2. 5 × 5 μm² AFM images of one-step grafting samples showing topography (left) and phase (right) with a Z scale of 30 nm and 50°, respectively, while typical RMS roughness is greater than 5 nm. The three different images shown represent binary brushes with different PS molecular weight: (a) PS1, (b) PS2, and (c), PS3 ($M_n = 28\,500$ g/mol).

0.75 ± 0.1 nm. Thicknesses of the grafted layers were averaged over several sample locations and detailed in Table 1. The index of refraction for the SiO₂, epoxysilane, PBA, and PS are considered constant and equal to the bulk values of 1.46, 1.429, 1.59, and 1.464, respectively.^{46–48} The contact angle was measured with a sessile drop method, using 2-μL droplets of Nanopure water, which were captured with a custom-built digital micro-

(42) Luzinov, I.; Julthongpipit, D.; Liebmann-Vinson, A.; Cregger, T.; Foster, M. D.; Tsukruk, V. V. *Langmuir* **2000**, *16*, 504.

(43) Tsukruk, V. V.; Luzinov, I.; Julthongpipit, D. *Langmuir* **1999**, *15*, 3029.

(44) Fisch, W.; Hofmann, W. *Macromol. Chem. Phys.* **1961**, *44–6*, 8.

(45) Motschmann, H.; Stamm, M.; Toprakcioglu, C. *Macromolecules* **1991**, *24*, 3681.

(46) Xie, R.; Karim, A.; Douglas, J. F.; Han, C. C.; Weiss, R. A. *Phys. Rev. Lett.* **1998**, *81*, 1251.

(47) Koneripalli, N.; Singh, N.; Levicky, R.; Bates, F. S.; Gallagher, P. D.; Satija, S. K. *Macromolecules* **1995**, *28*, 2897.

Table 2. Properties of the Grafted Layers

sample	polymer	thickness (nm)	RMS roughness (nm)	grafted amount (mg/m ²)	graft density (chains/nm ²)	interchain distance (nm)
1	First Step	0.58	NA	0.52	0.0483	5.14
	PBA 1 + PS 1	1.95 ± 0.2	0.23 ± 0.02	1.96	0.2809	2.13
2	First Step	0.94	NA	0.84	0.0782	4.04
	PBA 1 + PS 1	3.02 ± 0.2	0.19 ± 0.02	3.03	0.4342	1.71
3	First Step	0.87	NA	0.78	0.0724	4.19
	PBA 1 + PS 2	2.89 ± 0.2	0.18 ± 0.02	2.80	0.2592	2.22
4	First Step	0.9	NA	0.81	0.0749	4.12
	PBA 1 + PS 2	3.61 ± 0.3	0.20 ± 0.02	3.60	0.3336	1.95

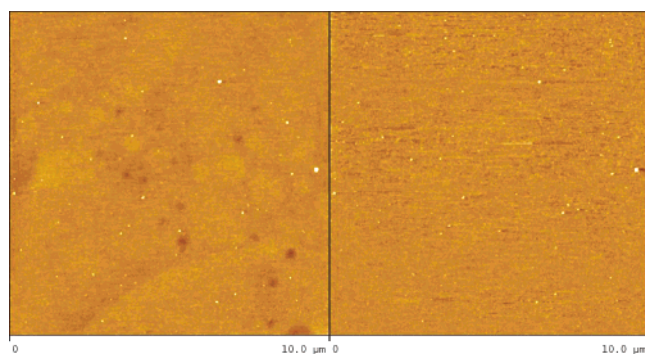


Figure 3. $10 \times 10 \mu\text{m}^2$ AFM images for sample 4 listed in Table 2 with topography (left, scale is 10 nm) and phase (right, scale is 20°) showing the typical clean, large-scale uniformity of the binary brush layer using the sequential, two-step grafting.

scope. Atomic force microscopy (AFM) (MultiMode and Dimension 3000, Veeco Metrology) was used for topographical and phase imaging in air according to the procedures adapted in our lab.^{49,50} Unless otherwise noted, all AFM images were obtained using the light-tapping regime, governed by the setpoint ratio (rsp), which is defined as the ratio of operating setpoint (amplitude) to the free oscillating amplitude of the cantilever. The attractive regime, or light-tapping, is characterized by an rsp of 0.9–1, while the repulsive regime, or hard-tapping, has an rsp of 0.4–0.7. In light-tapping, the tip sample interaction is strongly influenced by adhesion and the phase shift is greater on the surface with areas of higher attractive forces, whereas in the hard-tapping regime the elastic response becomes predominant.⁵¹ AFM tips were MikroMasch (Talin, Estonia) v-shaped, noncontact tips with a nominal spring constant ranging from 30 to 100 N/m. For the high-resolution (less than $1 \times 1 \mu\text{m}^2$) AFM imaging, care was taken to use a silicon tip with a radius less than 15 nm, which was determined by scanning a gold nanoparticle reference sample.⁵²

Switching of the Brushes. To examine the chain reorganization and kinetics of reversible switching of surface properties in the binary brush, samples were exposed to selective solvents for each component. Selective good solvents for the PS and PBA system are trichloroethylene (TCE) for PS and *n*-butanol for PBA. After hydrolysis, for the PS/PAA binary brush, toluene was used as the selective solvent for PS, while water heated to 75°C was used for PAA. Samples were immersed in solvents for varying amounts of time, dried quickly under dry N_2 , and contact-angle measurements were done within 5 min of solvent drying; the samples were quickly imaged with AFM.

Tribology Testing. A custom-built microtribometer, an oscillating friction and wear tester, was used to characterize the

(48) *Handbook of fine chemicals and laboratory equipment*; Aldrich: St. Louis, 2003. *Polymer Handbook*, 4th ed.; Brandrup, J., Immergut, E. H., Grulke, E. A., Eds.; John Wiley and Sons: New York, 1999.

(49) Ratner, B., Tsukruk, V. V., Eds. *Scanning Probe Microscopy of Polymers*; ACS Symposium Series 694; American Chemical Society: Washington, DC, 1998.

(50) Tsukruk, V. V. *Rubber Chem. Technol.* **1997**, *70*, 430.

(51) Magonov, S. N.; Cleveland, J.; Elings, V.; Denley, D.; Whangbo, M. H. *Surf. Sci.* **1997**, *389*, 201.

(52) Radmacher, M.; Tilmann, R. W.; Gaub, H. E. *Biophys. J.* **1993**, *64*, 735.

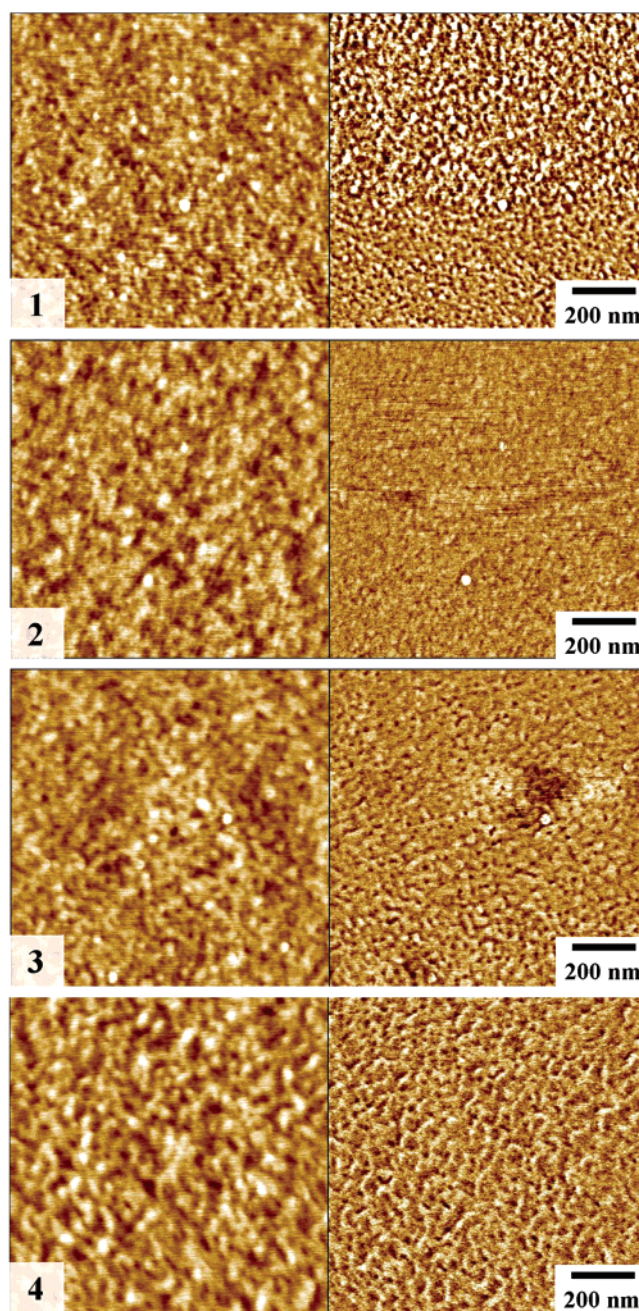


Figure 4. $1 \times 1 \mu\text{m}^2$ AFM images, topography (left, scale is 3 nm) and phase (right, scale is 20°). Numbers correspond to sample numbers in Table 2.

frictional characteristics of the mono and binary brush layers. A planar specimen with a polymer brush was mounted on a platform and oscillated against a stationary glass ball with a smooth surface (microroughness less than 1 nm as determined with AFM) with an applied load of $200 \mu\text{N}$, which corresponded

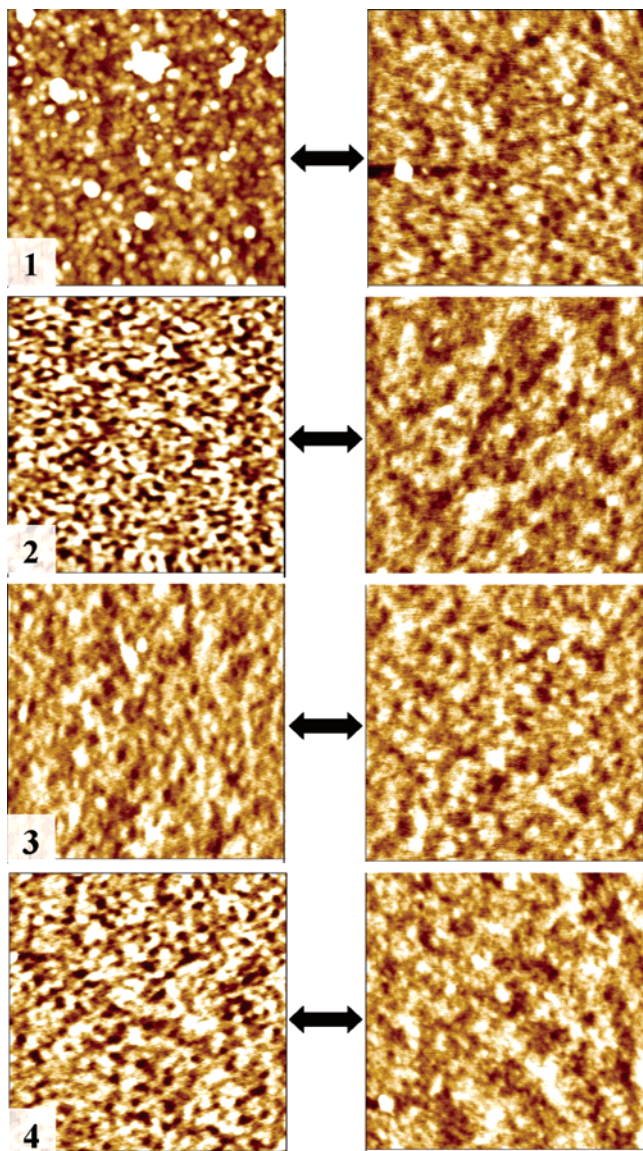


Figure 5. $400 \times 400 \text{ nm}^2$ topographical AFM images of different binary layers after exposure to *n*-butanol (left column) and TCE (right column). The Z scale for topography is 3 nm. The numbers correspond to sample numbers in Table 2.

to the maximum Hertzian pressure of 34.3 MPa. Prior to test, the glass ball was subjected to an ultrasonic cleaning in acetone and methanol solutions for 15 min each to remove organic contaminants and residual debris originated from the polishing process. The glass ball was then rinsed in deionized water for 5 min and dried by compressed nitrogen gas flow. The sliding speed was $330 \mu\text{m/s}$ and the stroke length was 1.6 mm. The tests were conducted at 5% and 80% relative humidity in ambient environment.

The chemical composition of the surface was probed with Auger electron spectroscopy (AES) on a PHI-670 instrument. AES surface analysis was performed using a field emission gun with an accelerating voltage of 5 kV and a current of $0.0185 \mu\text{A}$. The working potential for depth sputtering was 1 kV using Ar-ion. Under this working condition, the sputtering rate was $7 \text{ \AA}/\text{min}$ when calibrated against SiO_2 .

Results and Discussion

One-Step Grafting Synthesis. One-step grafting for the synthesis of the binary layer resulted in heterogeneous surface morphology, as shown in Figure 2. As can be seen, such a procedure leads to large surface-domain structures

in the resulting morphology, caused by phase separation during grafting. As known, when grafting two polymers simultaneously from a mixed solution, the polymers can aggregate in solution before grafting, as well as one being preferentially adsorbed onto the silicon, and the other dewetting the surface.^{53–55} Typical lateral dimensions of phase-separated surface areas were several hundred nanometers, with the surface microroughness exceeding 5 nm. Considering that we are focusing on the fabrication of surface layers with fine surface morphology, we concentrated mainly on the alternative sequential approach which produces desirable surface layers.

Two-Step Grafting Synthesis. The key to fabrication of binary polymer surfaces is to have control over the first step, in this case PBA. Allowing this first reaction to continue for too long will result in the majority of the grafting sites being consumed, meaning that the second polymer (PS) will not be able to penetrate through the adsorbed PBA chains. Prematurely terminating the reaction will have the opposite effect in which the binary layer will be highly asymmetric in favor of PS. When the brush binary layer is symmetric in terms of the grafted amount, it enhances the switching in surface composition of the layer.⁵⁶

For the four samples studied here, we grafted PBA at the first step because the grafting of PS followed by PBA produced unstable results. The amount of PBA grafted onto the surface was controlled by altering the grafting (annealing) time and temperature. In a previous publication, we have fully characterized the kinetics of PBA layer formation.⁵⁷ The kinetics of layer formation for PBA revealed that half of the full achievable thickness occurs around 20–30 min, thus, we chose 20 min as the grafting time and varied the temperature, as indicated in Table 1.⁵⁷ For comparison, the theoretical maximum thickness for the PBA used in this work ($M_n = 6500 \text{ g/mol}$) is $h = 3.3 \text{ nm}$, based upon well-known polymer brush models.^{16,57,58} Thus, we have chosen our PBA grafting conditions using this model. We have characterized the grafting kinetics of both PBA and PS and observed that the grafting conditions are highly reproducible.⁵⁷

Surface Layer Properties. The parameters of the grafted layers are listed in Table 2. The grafting density (\mathbf{D} , chains/ nm^2) of the brush layers was evaluated from M_n and the layer thickness (\mathbf{d} , nm) according to the formula: $\mathbf{D} = d\rho N_a / (M_n \times 10^{21})$, where ρ (g/cm^3) is the density of the polymer and $N_a = 6.022 \times 10^{23}$ (mol^{-1}) is Avogadro's number.⁵⁹ The anticipated average distance between grafting points, \mathbf{l} , is calculated as $\mathbf{l} = 2(\pi\mathbf{D})^{-0.5}$. An indication of having polymer brush surfaces can be when the interchain distance is less than the radius of gyration of the corresponding free polymer chain.¹⁴ For PS1, PS2, and PBA, the radius of gyration has been calculated as 1.80, 2.73, and 2.24 nm, respectively.⁵⁷ We have achieved high grafting densities for all samples, and the overall interchain grafting distance in all cases (except sample 1, with a difference of 0.33 nm) is less than the radius of gyration of these PS and PBA free polymer chains

(53) Henn, G.; Bucknall, D. G.; Stamm, M.; Vanhoorne, P.; Jerome, R. *Macromolecules* **1996**, *29*, 4305.

(54) Higgins, A. M.; Jones, R. A. L. *Nature* **2000**, *404*, 476.

(55) Lu, G.; Li, W.; Yao, J. M.; Zhang, G.; Yang, B.; Shen, J. C. *Adv. Mater.* **2002**, *14*, 1049.

(56) Minko, S.; Luzinov, I.; Luchnikov, V.; Müller, M.; Patil, S.; Stamm, M. *Macromolecules* **2003**, *36*, 7268.

(57) Julthongpipit, D.; LeMieux, A.; Tsukruk, V. V. *Polymer* **2003**, *44*, 4557.

(58) Siqueira, D. F.; Kohler, K.; Stamm, M. *Langmuir* **1995**, *11*, 3092.

(59) Luzinov, I.; Julthongpipit, D.; Malz, H.; Pionteck, J.; Tsukruk, V. V. *Macromolecules* **2000**, *33*, 1043.

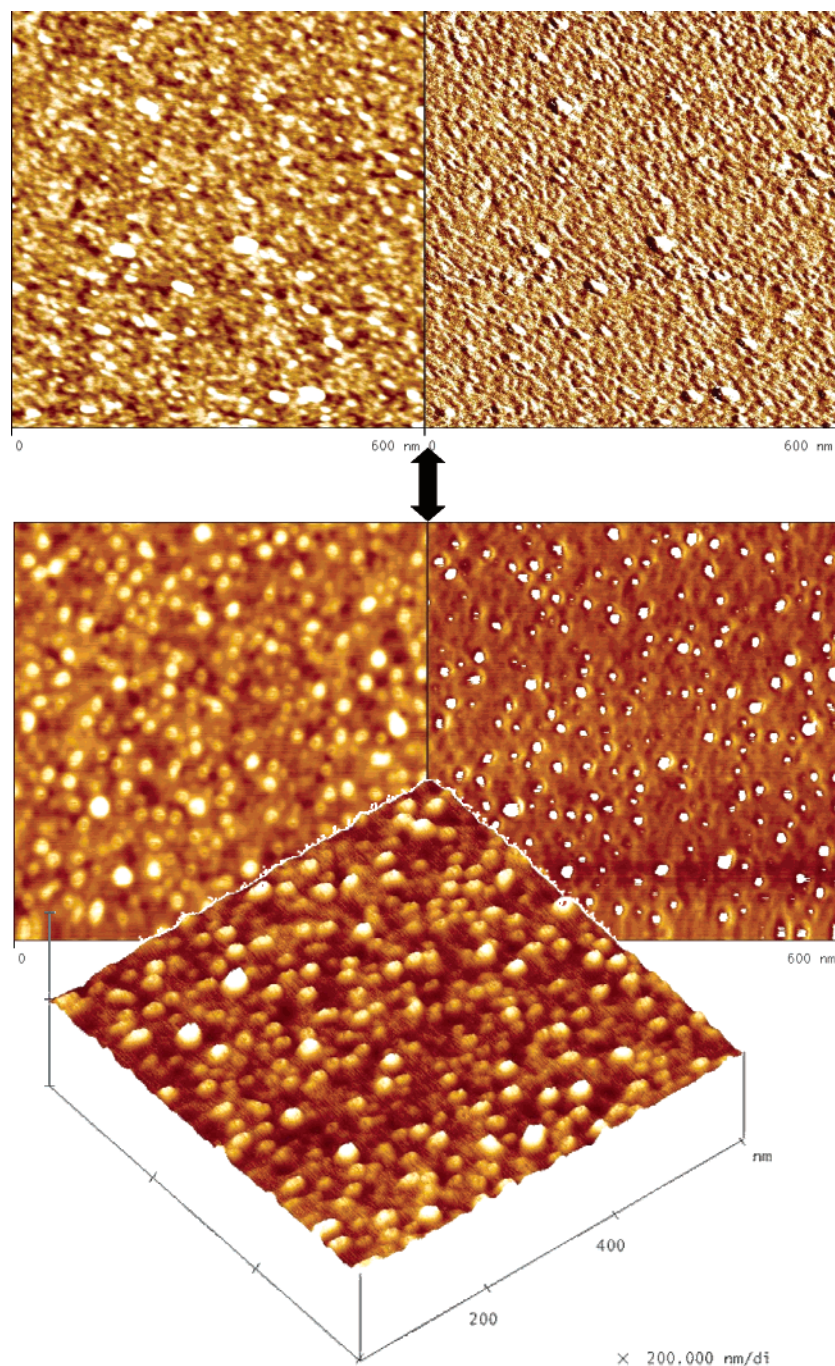


Figure 6. $600 \times 600 \text{ nm}^2$ AFM images for sample 3 (Table 2), topography (left) and phase (right), demonstrating switching after PBA hydrolysis to PAA. The top image is after exposure to toluene, the middle is after water exposure, and the bottom is a 3D image of the binary layer after water exposure. The Z scale for topography is 5 nm and 20° for phase.

in solution, indicating that the chains are indeed in a stretched, brushlike conformation. This is summarized in Table 2 where the overall grafting distance considers both PS and PBA chains.

Large-scale representative AFM images of the as-grafted binary surface layer obtained in a two-step approach from toluene solutions shown in Figure 3 demonstrate overall uniformity of the surface layer without large-scale bumps and holes, indicating dewetting, microscopic phase separation (compare with Figure 2), or contamination. All binary surface layers have a fine nanostructured surfaces with phase sizes and interdomain spacing not more than a few tens of nanometers, as can be seen on high-resolution AFM images (Figure 4). The surface RMS surface roughness does not exceed 0.3 nm,

which is far less than the size of the free polymer chain, indicating extremely homogeneous and uniform surfaces (Table 2). Higher molecular weight of the PS component and higher grafting density resulted in a slightly better defined domain morphology of binary layers.

The binary brush layer was immersed in TCE (good selective solvent for PS) and *n*-butanol (a good selective solvent for PBA) for 2 h and rapidly dried so that the morphology under solvent is effectively frozen and retained in the dry state since the time for chain reorganization is much slower than solvent evaporation.²⁸ Figure 5 shows high-resolution AFM images of the binary brush surface after exposure to different selective solvents, demonstrating some subtle changes in surface morphology. The contact angle changed from 93° after TCE exposure to 80°

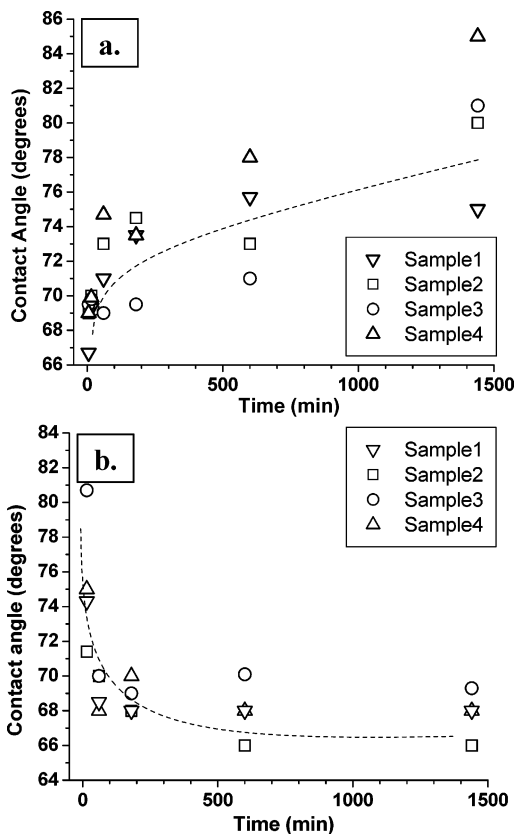


Figure 7. The kinetics for switching of surface wettability after toluene (a) and water (b) treatments, as measured by contact angle, for the binary brush layers (sample numbers correspond to Table 2) after hydrolysis. The time indicates the time immersed in solvent before measurement. The dashed lines are guides for the eye.

after *n*-butanol exposure, which is very close to the values for pure PS and pure PBA, respectively.⁴⁸ However, this

contact-angle change is small due to the modest difference in amphiphilicity of PS and PBA chains. To amplify and to better observe the changes in surface morphology, we conducted hydrolysis of PBA chains and their conversion to PAA chains (Figure 1).

Treatment of PS–PAA binary brush layers in different selective solvents resulted in dramatic reorganization, as seen in AFM images showing the switching of morphology after exposure to toluene and water (Figure 6). The weakly ordered domain structure after toluene treatment is replaced with a well defined, dense packing of circular domains with a 20–30-nm diameter after treatment with water. These lateral dimensions, much smaller than that typically observed for thick brush layers, result from the relatively low molecular weight and modest grafting density. The AFM tip instability on the top of these domains, due to tip interaction with more than one material simultaneously, resulted in apparent depletions of the tops and sharp change in phase contrast. This behavior indicates complex structure of the narrow domains with different composition in the center portion and along the edges of the domains, as was suggested for PS–PAA Y-shaped brushes.^{38,39} Reorganization of surface morphology with predominant surface location of either PS or PAA chains resulted in more-significant changes in the surface wettability than recorded for PS–PBA layers with the contact angle changing from 60–65° to 85–90° in selective solvents (Figure 7). These contact-angle changes of 15–20° for different binary brushes occur within the initial 100 min of treatment (Figure 7).

Preliminary Studies of Tribological Properties.

Tribological properties are greatly affected by the presence of a thin polymeric surface layer with different chemical compositions and surface functionalities, as demonstrated in Figure 8. The friction coefficient determined from repeating reciprocate sliding cycles is virtually constant

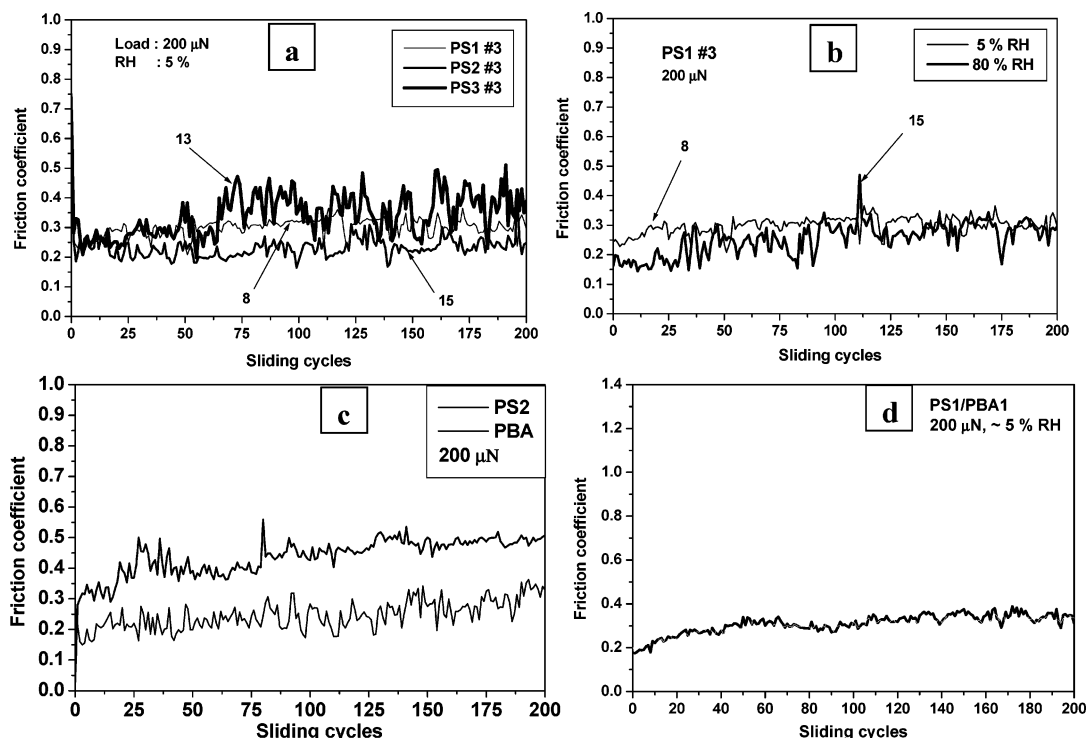


Figure 8. Friction coefficient versus number of sliding cycles for grafted PS # layers of different molecular weights at a low humidity of 5% (a); for a grafted PS 1 layer at different humidity (b); for PS 2 and PBA layers at low humidity (PBA data are higher) (c); and for sample 1 (Table 2) of binary brush layer (d).

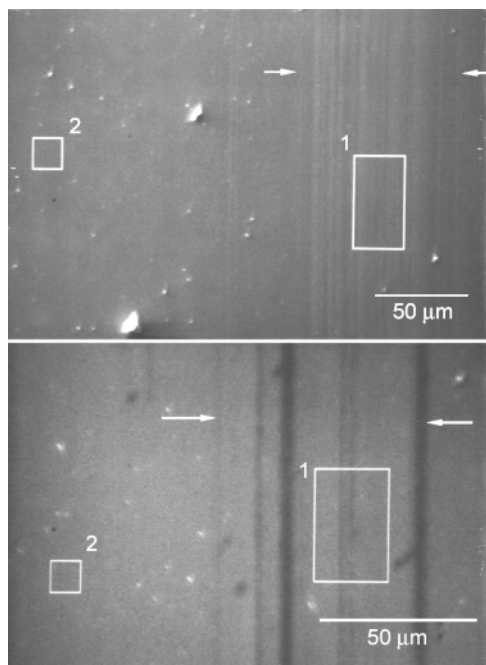


Figure 9. SEM images of intact and worn surface areas (vertical track on a right side as indicated by arrows) for PS 1 (top) and PBA (bottom) grafted layers. Rectangular shapes show selected areas for AES analysis.

for the hydrophobic glassy PS surface layers with different molecular weight and varies within 0.2–0.3 at low humidity (5%) with the lowest friction coefficient observed for PS3 coating (Figure 8a). Increasing humidity resulted in lowering of the friction coefficient, especially in the initial stage (for a number of cycles below 100) to below 0.2 that indicates an importance of the presence of a thin water layer, even on a hydrophobic glassy surface of the PS layer (Figure 8b). The friction coefficient was higher for the rubbery surface layer of PBA, reaching 0.38–0.44 for a higher number of cycles at low humidity (Figure 8c)

and even higher for increasing humidity (not shown). Both values are fairly similar to that observed for glassy and rubbery bulk polymers in macroscopic testings and usually related to both stronger polar interactions and larger contact areas for rubbery materials.⁶⁰

However, despite a higher friction coefficient, the grafted PBA rubbery layer with a thickness of about 3 nm is much more wear resistant than the corresponding glassy layer. In fact, the worn track is less regular in PS-coated silicon than in corresponding PBA-coated silicon, where no deep grooves have been observed on SEM images (Figure 9). Moreover, the Auger electron spectroscopy shows a striking difference in the wearing behavior of these surface layers (Figure 10). The original depth profile of all major chemical elements was very different for PS and PBA layers. The carbon concentration was the highest at the surface for the PS layer, indicating a full coverage of the silicon surface with PS chains, as was concluded from AFM data (Figure 10a). Oxygen concentrated mainly in the middle portion due to the presence of the silicon oxide layer of 1.1 nm, as calculated from ellipsometry. Unlike for the PBA layer, significant oxygen presence was found directly on the surface due to the high concentration of carboxylic groups in PBA backbones (Figure 10b). Wearing down the PS layer resulted in dramatic changes of the chemical composition, indicating significant deterioration of the PS layer and presence of oxidized polymer material and the exposed silicon oxide layer (Figure 10c). In contrast, signs of oxidation or the coating removal could not be found for the rubbery coating: the chemical composition of the PBA layer within the contact areas did not change at all, as can be seen from element profiles in Figure 10d. Thus, this layer demonstrated a high recovery ability and a restoration of its initial microstructure after being subjected to high normal and shear stresses due to large reversible elastic deformations of polymer chains below the glassy state.⁶¹

Finally, for the binary surface layer, we observed very stable friction behavior at low humidity, with the friction coefficient being very stable and low (within 0.2–0.3)

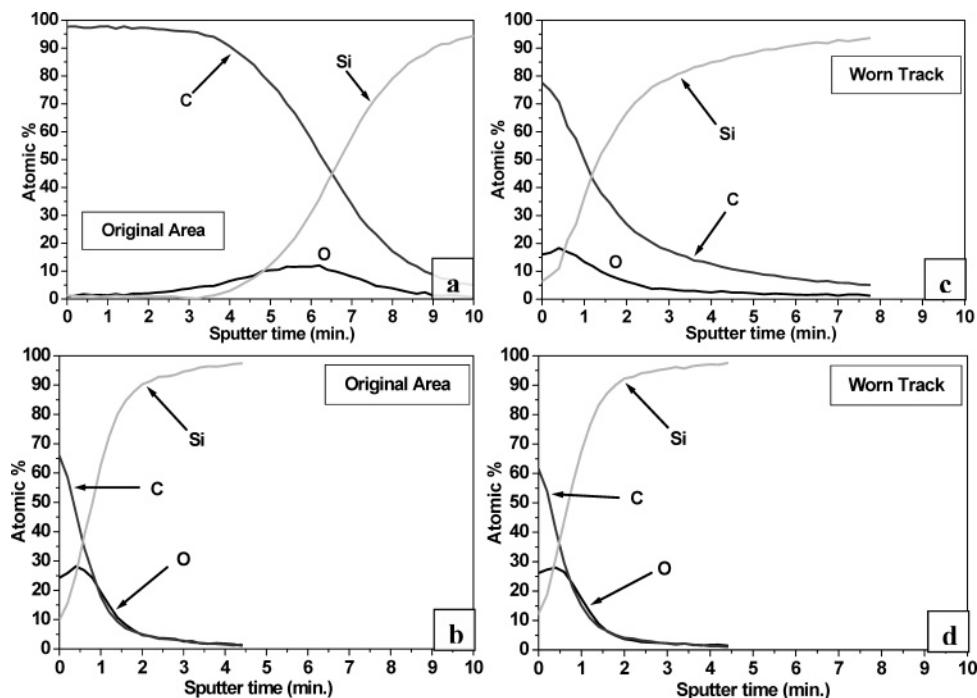


Figure 10. Auger analysis of an original, undamaged surface (a,b) compared with the worn areas (c,d) of the respective PS (a,c) and PBA (b,d) brush layers. The depth profile of C, O, and Si are shown in time-scale.

despite the presence of rubbery phase (Figure 8d). The stability of the binary coatings can be associated with the presence of both the stiff, glassy microphase bearing the normal load and the rubbery domains providing elastic recovery. However, increasing humidity resulted in fast

(60) Bhushan, B., Ed. *Micro/Nanotribology and Its Applications*; Kluwer Academic Publishers: Dordrecht, The Netherlands, 1997. Luzinov, I.; Julthongpiput, D.; Gorbunov, V.; Tsukruk, V. V. *Tribol. Int.* **2001**, *34*, 327.

(61) Tsukruk, V. V. *Adv. Mater.* **2001**, *13*, 95.

damaging of the binary coating due to increasing capillary forces, as will be further addressed in forthcoming studies.

Acknowledgment. This research is supported by the National Science Foundation (Grant No. CMS-0099868) and The National Research Laboratory Program of the Korean Ministry of Science and Technology. The authors thank Sergiy Peleshanko for worthwhile discussions and technical assistance.

LA048496B